

Automatic Liver Segmentation using the Random Walker Algorithm

F. Maier^{1,2}, A. Wimmer^{2,3}, G. Soza², J. N. Kaftan^{2,4}, D. Fritz^{1,2}, R. Dillmann¹

¹Universität Karlsruhe (TH),

²Siemens Medical Solutions, Forchheim,

³Friedrich–Alexander University Erlangen–Nuremberg,

⁴RWTH Aachen University

maier@ira.uka.de

Abstract. In this paper we present a new method for fully automatic liver segmentation in computed tomography images. First, an initial set of seed points for the random walker algorithm is created. In this context, voxels belonging to air, fat tissue and ribcage are labeled as background. Furthermore, depending on the shape of the ribcage and voxel intensities, several seed points inside the liver are automatically selected as foreground. This seed mask is then used to initialize the segmentation algorithm. Our method was successfully tested on data of 22 patients.

1 Introduction

Liver segmentation is an important prerequisite for a variety of applications. Surgery planning, image guided liver surgery and computed tomography (CT) perfusion examinations benefit from an accurate segmentation.

Fully automatic and at the same time accurate liver segmentation is an unsolved problem by now, despite several diverse attempts exist. Soler et al. [1] presented an algorithm for a segmentation of the liver using a reference 3-d model. After estimation of the liver contour, the model is improved by means of topological and geometrical analysis. With this approach, however, the segmentation is constrained by the reference model, which can be adapted to the real image information only in a restricted way. Lamecker et al. [2] presented an approach for liver segmentation using a 3-d statistical shape model built from a training set of semi-automatically segmented livers. This technique also suffers from restricted flexibility in shape adaptation. Lim et al. [3] use their deformable contour model for segmentation.

A drawback common to most approaches is a lack of interactive controllability if the automatic segmentation has failed. Grady et al. [4, 5] introduced the random walker (RW) algorithm, which is a general segmentation technique based on graph theory. It allows image segmentation given fore- and background seed points. A big advantage of the algorithm is that the calculated results can be easily corrected in a semi-automatic way.

2 Materials and Methods

A new fully automatic algorithm for liver segmentation is introduced. The presented algorithm extends and adapts the general graph theoretic image segmentation [4] to the liver segmentation problem. Within our approach, several seed points inside and outside of the liver are automatically detected. These seeds are then supplied as input to the RW algorithm.

2.1 Generation of seed points

In the first step, seed points within different abdominal structures are automatically detected. All seed points lying within structures outside the liver are then labeled as background and seed points within the liver are labeled as foreground. Seed point detection is performed for each slice separately. A polar coordinate system is associated with each axial slice. The center of the polar coordinate system is set to the barycenter of the body. The advantage of such a polar coordinate system is that the angle coordinate can be easily correlated with the anatomy to make restrictions which part of the body can comprise the liver (e.g., left, right, anterior, posterior, see Fig. 1(a)).

Several different structures are considered for automatic seed detection. The details are provided below.

Generation of ribcage seed points To prevent oversegmentation of the liver into the adjacent muscle tissue between the ribs, the shape of the ribcage is estimated. For this purpose, anatomical knowledge is used. First assumption is that the liver is located on the right side of the body near the bottom of the ribcage. It is also assumed that some liver tissue touches or is very close to the ribcage. The rib detection algorithm works as follows.

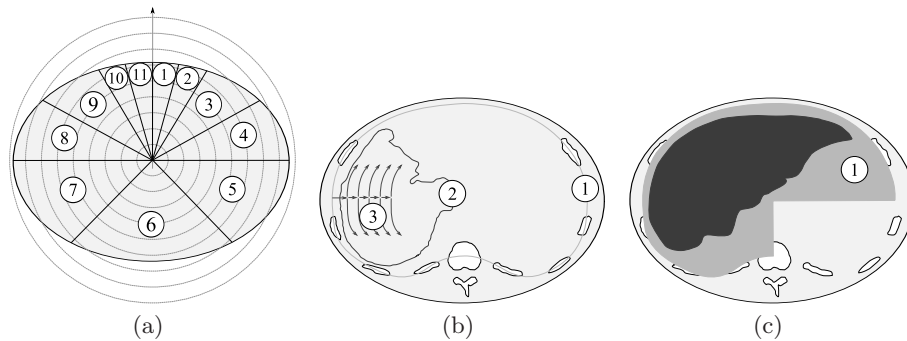


Fig. 1. Segmentation: (a) Polar coordinate system and angle depended sector sizes. Anterior: small sectors (1, 2, 10, 11), posterior: large sector (6). (b) Liver seed point creation. Spline (1), contour of liver (2), liver seed search paths (3). (c) Histogram analysis area (1). The area for histogram analysis is defined by the interior of the ribcage spline in the posterior and anterior right part of the abdomen

First, intensity differences on each radius for all angles are checked to detect the body surface and the boundary between fat and muscle tissue (Fig. 2(a)). Median filters with angle dependent kernel sizes are applied to all determined radii in order to eliminate outliers. Based on the detected boundary and an angle dependent maximum rib depth, a search area is defined (Fig. 2(b)). Voxels therein with high intensities (e.g., > 300 HU) are classified as bone (Fig. 2(c)). Positions of ribs are stored in a separate list (Fig. 2(d)). Then, all detected rib positions are clustered with hierarchical clustering depending on radius and angle of the voxel positions belonging to the ribs. The final cluster centers are stored as the outer rib positions, one for each rib (Fig. 2(e)).

Starting with the outer rib positions, the corresponding inner rib positions are estimated by analysis of the intensity profile into the direction of the body barycenter (Fig. 2(f)). The inner rib positions shifted away from the body center by some small safety distance are used as support points for a cubic spline (Fig. 1(b)). If there are not enough support points in a given sector (Fig. 1(a)), positions from neighboring slices are used. In this case, a new rib point is placed into the current slice by interpolating the corresponding lower and upper rib positions. If there are no rib points that can be used, points from the fat/muscle boundary are taken as substitute. This prevents the spline from passing through the liver. The ribcage points lying on the generated spline curve are taken as background seeds for each slice. This information prevents the RW algorithm from oversegmentation of the liver into the surrounding muscle or fat regions.

Generation of liver seed points An intensity histogram is built from voxels in the anterior and right posterior part of the abdomen that are enclosed by the cubic spline (Fig. 1(c)). Known background voxels like air, fat or bone are thereby excluded. HU value distributions of the liver and stomach are assumed to be Gaussians. Hence, mean and variance of these Gaussians are estimated by a bimodal distribution analysis. Mean and variance of the Gaussian of the liver are used to define the intensity range of liver pixels. On the right side of the body

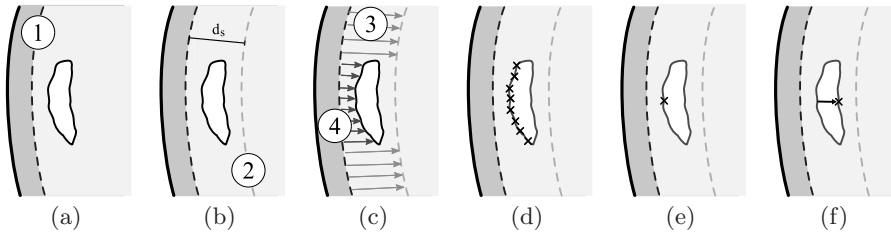


Fig. 2. Rib detection: Right part of the body including fat tissue (dark gray) and rib (white). (a) Fat/muscle boundary (line 1). (b) Maximum search depth d_s (line 2) from fat/muscle boundary. (c) Search for bone failed on bright paths (3). Search was successful on dark paths (4). (d) Marked points: detected outer bone positions. (e) Marked point: Center of bone position cluster, outer rib position. (f) Marked point: Inner rib position, corresponding to outer position of (e) detected on search path

the right turning point of the spline is used to start foreground seed generation (Fig. 1(b)). The radius is reduced in given steps and the corresponding pixels are checked if they lie within the range calculated from the histogram. If they fulfill this criterion, they are labeled as foreground seeds. The angle is then changed iteratively in the clockwise and counter-clockwise direction. The progression of each line will stop if a group of pixels is outside the intensity interval or a stop position is reached. Stop positions are defined by the last visible rib.

Generation of air, bone and fat seeds Air and any other gases are clearly delineated in CT data and are used to generate background seeds. All voxels with a lower intensity than a predefined threshold (e.g., -460 HU) are marked as air. All voxels with a higher intensity than a given threshold (e.g., 325 HU) are classified as bone. Fat tissue inside the body is also labeled as background. For this purpose, the image is first filtered with a median filter (e.g., 9×9 pixel), which reduces noise. After filtering, an interval threshold (e.g., -117 HU to -53 HU) is applied and the result is classified as fat tissue.

3 Results

In order to prove the stability of the method with respect to varying liver shapes and contrast enhancements, the algorithm has been evaluated with 22 CT liver perfusion datasets comprising native, arterial and venous enhancement phases. Since perfusion scans require a high temporal resolution, they are acquired without CT table movement. The maximum number of slices is consequently limited by detector width and reconstruction settings and was less or equal 12 in our experiments. Slice distance and slice thickness were equal in all datasets and varied between 2.4 and 6 mm. The axial resolution of all slices was 512×512 voxels of size varying between $0.64 \times 0.64 \text{ mm}^2$ and $0.72 \times 0.72 \text{ mm}^2$.

The automatic results have been quantitatively compared to manual segmentations performed by medical experts using the dice similarity coefficient (DSC), the average contour distance (\bar{d}) and the Hausdorff distance (H). Mean values and standard deviations over all 22 patients are $\mu_{DSC} = 91.9\%$, $\sigma_{DSC} = 7.2\%$, $\mu_{\bar{d}} = 4.6$ mm, $\sigma_{\bar{d}} = 3.7$ mm, $\mu_H = 34.3$ mm and $\sigma_H = 14.53$ mm. Table 1 shows more detailed numerical results for seven randomly selected patients. Additionally, visual analysis of the segmentation results has been conducted, which confirmed the overall good quality of the results. The resulting liver contours and probabilities for each voxel to be part of the liver are presented in Fig. 3.

Execution of the RW algorithm on downsampled (256×256) 3-d images required between 1.63 s (1 slice) up to 19.56 s (12 slices) on an Intel Pentium 4 CPU (3.4 GHz, 1 GB RAM). The seed point creation algorithm needed 7.7 s per slice. The software has been developed with MeVisLab 1.4 (VC++ 6).

Table 1. Results: dataset (D), vol. of dataset (V), vol. of RW segmentation (RWV), vol. of manual segmentation (MV), vol. of overlap (OLV), vol. of oversegmentation (OSV), vol. of undersegmentation (USV), all volumes in ml, \bar{d} , and H in mm

D	V	RWV	MV	OLV	OSV	USV	DSC	\bar{d}	H
1	1075,8	155,1	147,9	145,6	9,5	2,3	96,1%	2,1	14,2
2	3232,1	439,6	441,4	394,1	45,5	47,3	89,5%	5,9	36,9
3	3465,6	778,6	771,7	760,3	18,3	11,3	98,1%	1,7	56,0
4	3270,8	606,2	662,8	585,0	21,1	77,8	92,2%	5,4	49,4
5	3232,1	769,9	757,1	731,8	38,1	25,3	95,9%	1,7	13,5
6	3290,2	279,8	256,4	238,1	41,7	18,3	88,8%	4,4	28,8
7	3270,8	675,2	695,8	637,5	37,8	58,4	93,0%	5,3	47,5

4 Discussion

In this paper, a fully automatic liver segmentation algorithm, based on the general RW approach and customized automatic seed point creation, has been proposed. Using the presented approach, it is possible to generate robust liver segmentations. There are only few assumptions about the shape and size of the liver. Therefore, it is possible to reach high segmentation quality on abnormal livers, in contrast to model based approaches. Small intensity differences, caused e.g. by liver tumors, do not corrupt the segmentation results.

The segmentation algorithm reaches an average DSC value of 91.9%, which shows the high concordance between automatic and manual segmentation. The large mean value of H is caused by oversegmentation of small areas between the lobes of the liver. Oversegmentation of these small gaps causes high peaks in the surface distance between manual and automatic segmentation. The significantly lower value of \bar{d} shows that most of the distances between the surfaces are smaller than the peaks. In difficult cases, the new algorithm allows intuitive interactive correction of its results. Users that are capable to use a simple paint application will be able to quickly edit the results in a semi-automatic way.

Improvements of our approach can be attained by integrating additional background seed points using existing organ segmentations (e.g., heart). Furthermore, a more efficient implementation of the seed point creation algorithms would bring improvement in execution times.

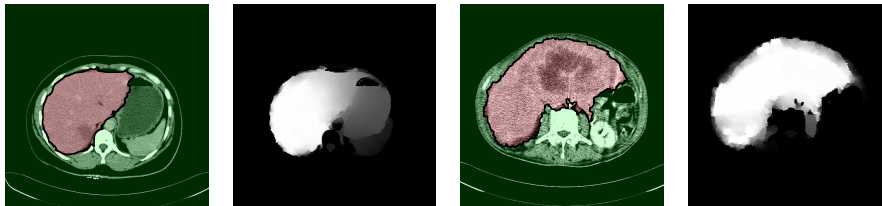


Fig. 3. CT image slices with determined liver contours (black) and corresponding probabilities (white=100%, black=0%)

References

1. Soler L, Delingette H, Malandain G, et al. Fully automatic anatomical, pathological, and functional segmentation from CT scans for hepatic surgery. *Comput Aided Surg.* 2001;6:131–42.
2. Lamecker H, Lange T, Seebaß M. A statistical shape model for the liver. *Proc MICCAI.* 2002;2489:421–27.
3. Lim SJ, Jeong YY, Ho YS. Segmentation of the liver using the deformable contour method on CT images. *Proc SPIE.* 2005;3767:570–81.
4. Grady L. Random walks for image segmentation. *IEEE Trans Pattern Anal Mach Intell.* 2006;28(11):1768–83.
5. Grady L, Schiwietz T, Aharon S, et al. Random walks for interactive organ segmentation in two and three dimensions: Implementation and validation. *Proc MICCAI.* 2005;3750:773–80.